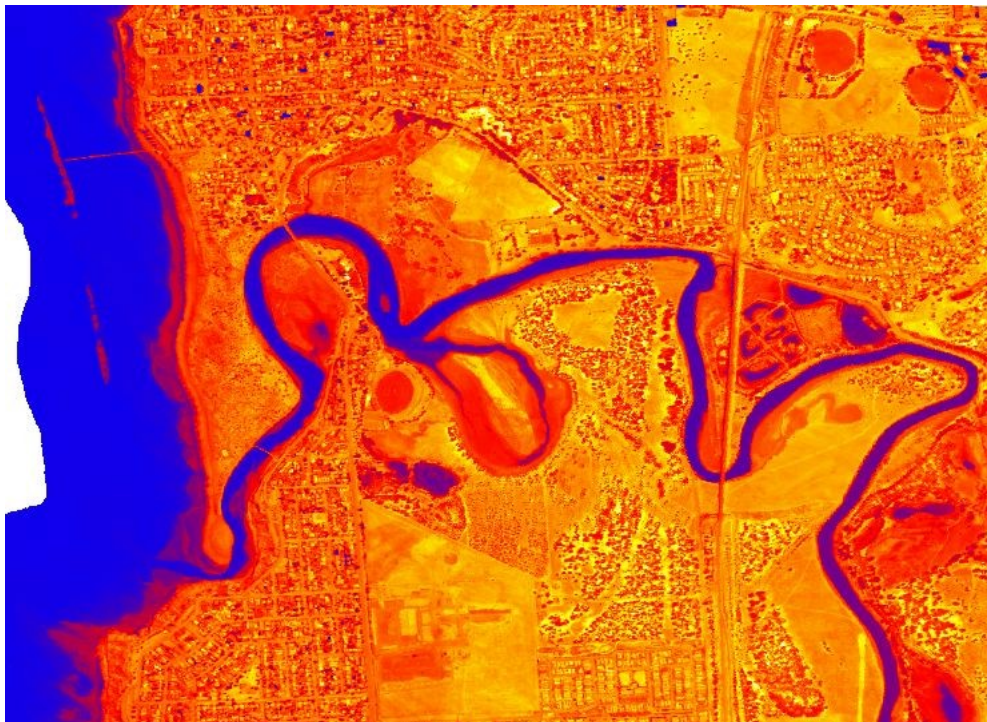




DEW Project: Adelaide Metro Thermal 2022 Project Report

Part B – Southern Area, collected January 2023



Version 1.1 March 2023

Table of Contents

1. Introduction.....	3
2. Survey area.....	4
3. Instrumentation and equipment.....	5
4. Project plan.....	5
5. Survey activity and Flight reports.....	6
5.1. 6-January– South subregion.....	6
6. Data processing.....	6
6.1. Project metadata.....	6
7. Data validation and context.....	8
7.1. Synoptic situation.....	8
7.2. Comparison data.....	9
7.3. Australian Bureau of Meteorology Automatic Weather Stations.....	9
7.4. Australian Bureau of Meteorology ACCESS-G Model output.....	9
7.5. Assessment of Thermal accuracy.....	11

1. Introduction

This report forms a supplement to, and should be read in conjunction with “DEW Project: Adelaide Metro Thermal 2022 Project Report Version 1.0 October 2022” (referred to in this Part B report as “the first delivered project report”), which details the planning, data collection and processing of a thermal imaging survey of the greater Adelaide metropolitan region, by Airborne Research Australia and begun in March 2022 for the South Australian Department of Environment and Water. This project aims at using a thermal imaging camera to map surface temperatures at high resolution in warm to hot conditions, both day and night.

The unusually cool and cloudy summer of 2021/22 did not provide sufficient suitable weather to complete the survey, and this report (“Part B”) adds description of the remaining, southern area capture conducted in early January 2023 to complete the survey.

Report by Andrew McGrath and Gustavo Cao Cancio.

Data collection by Andrew McGrath and Sharon Drabsch

Data processing by Andrew McGrath and Gustavo Cao Cancio, including analysis by Caecilia Ewenz.

2. Survey area

As described in the first delivered project report, the project targets the greater Adelaide metropolitan area from Gawler in the north to Sellicks Beach in the south, and from the coast to the start of the Mount Lofty Ranges.

Illustration 1 below shows the subdivisions of the area, of which all but the southern subregion were covered in the first stage of the project. This report, therefore, deals only with the South subregion.

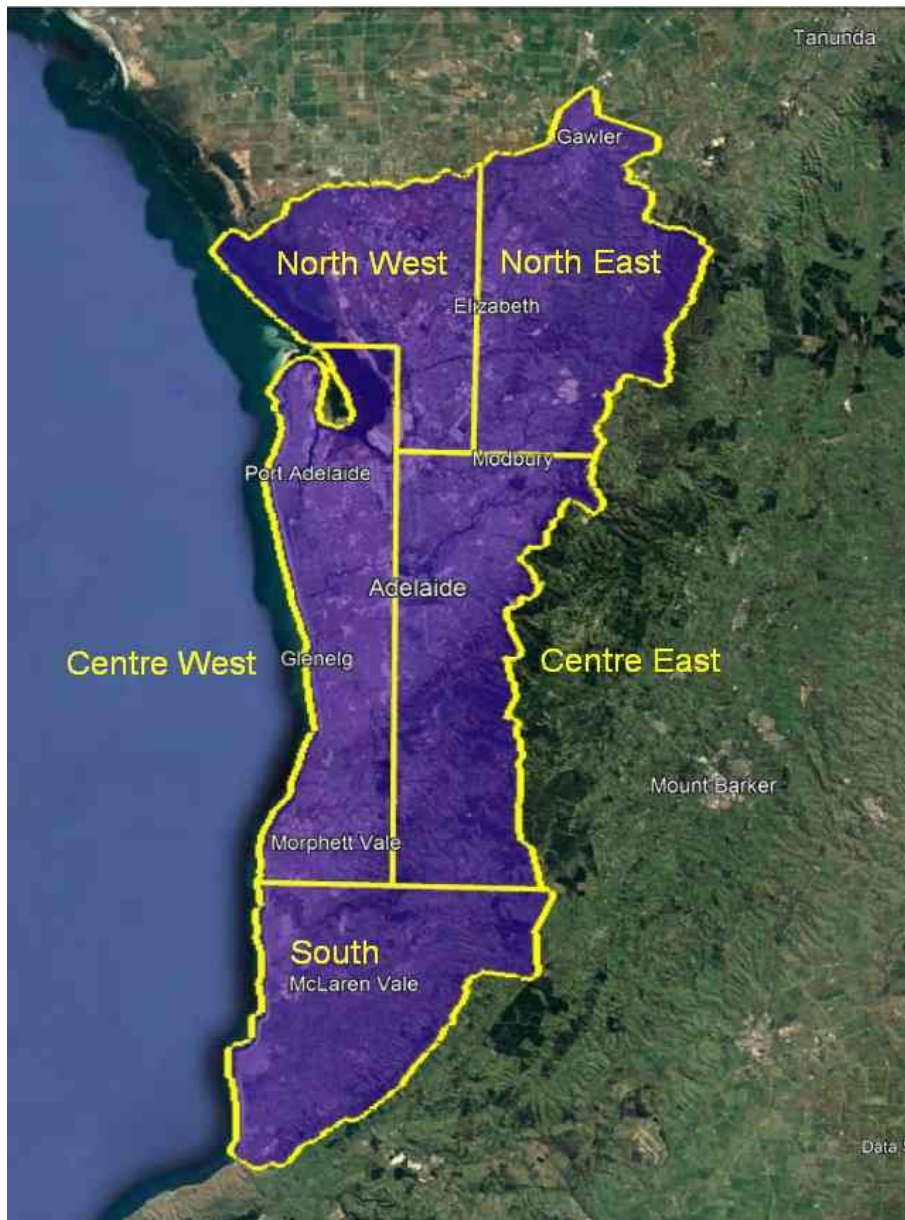


Illustration 1: Division of overall survey region into subregions achievable in a single day/night of flying. Subregion names are shown in yellow.

3. Instrumentation and equipment

The instrumentation and equipment used for this residual part of the overall survey are identical to that used and described in the first delivered project report.

4. Project plan

Based on the area specification above, ARA prepared a flight plan consisting of a grid of parallel lines to cover the areas with a 900m line spacing to ensure full overlap of swaths for all instruments. As can be seen in the illustrations below, this required a total of 30 flight lines across the South subregion.

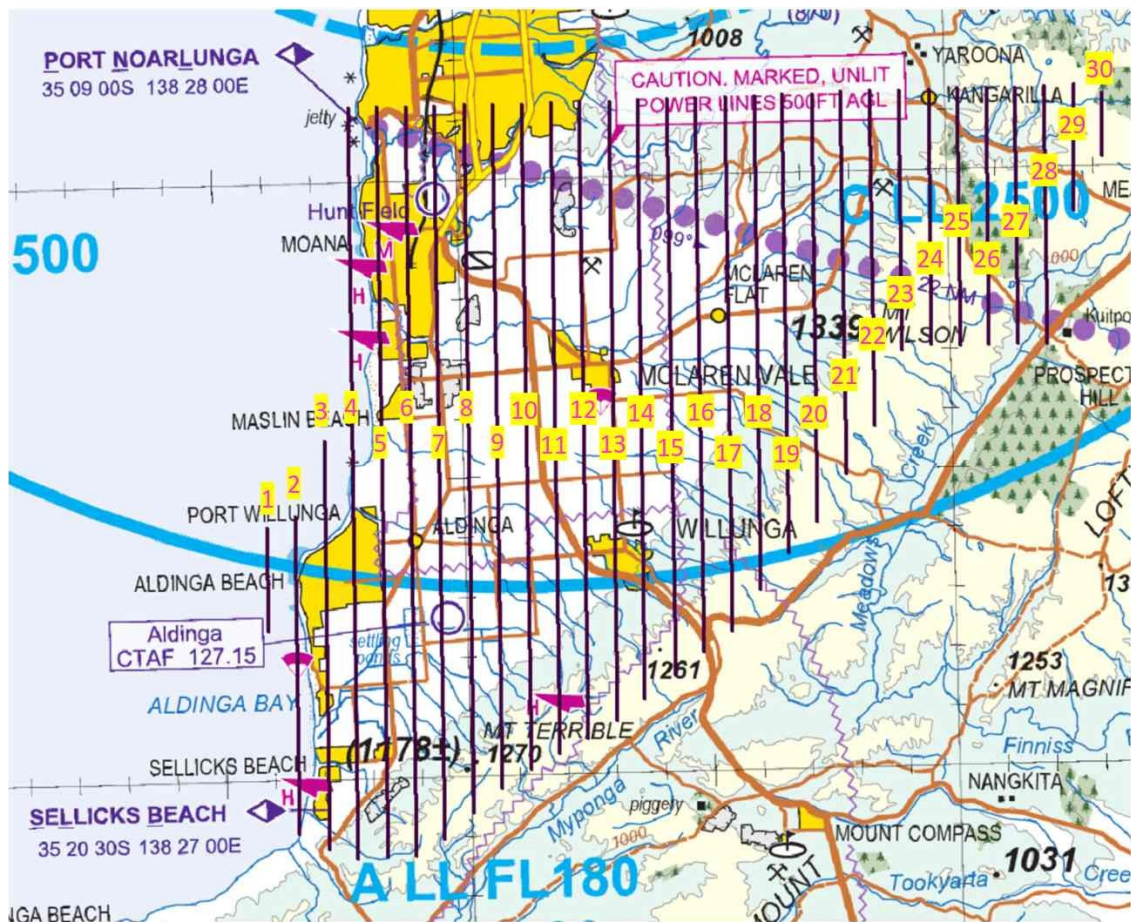


Illustration 2: Flight lines at a 900m line spacing to cover the "South" subregion, overlaid on the relevant aviation chart from the Civil Aviation Safety Authority.

A minor difference from the central and northern subregions described in the first delivered project report was that the lines were planned to be flown at a nominal 3600m altitude, to accommodate the larger areas of elevated terrain in the South subregion.

Additionally, because the 2022 failure of the panchromatic imager meant the the albedo product was derived instead from the hyperspectral data for the first survey, a decision was made to use the hyperspectral data for this purpose again, for consistency.

The 2022/23 summer season was affected by the near-unprecedented continuation of La Nina conditions into a third consecutive year, and opportunities for suitable periods of weather were again limited, although near-ideal conditions very similar to those under which the rest of the survey area had been captured, eventuated in early 2023 and the data capture was completed.

5. Survey activity and Flight reports

5.1.6-January– South subregion

The data collection flights were undertaken on the day and night of the 6th of January in good meteorological conditions (clear skies, low winds), taking off at approximately 10:30 local time for the daytime flight and a little before 11pm for the nighttime. Max BOM-observed temperature at West Terrace was 28.9°C, highly comparable with the maximum daily temperatures for the previous captures: 29.1, 33.7, 26.5 and 29.5°C.

All instrumentation apparently operated without fault for these two ~5-hour flights.

6. Data processing

The first delivered project report provides a detailed description of the processing workflow, and the data for the South subregion was processed in the same manner.

6.1. Project metadata

Although not a primary project outcome *per se*, the navigation data is provided as metadata supporting the imagery deliverables. For each of the measurement flights, a full-resolution .csv file is provided, giving IMU location and orientation at 4ms intervals.

Metadata detailing all flight tracks, including 5-second reports of aircraft altitude and the time-of-day, are provided in the form of KMZ flight track files on the provided data delivery disk. These are all in the directory

drive:\Nav-metadata

and have names identifying the date and time of the start of the navigation file.

Also provided in the same directory are high temporal resolution (250Hz) .csv files of final-accuracy IMU position and orientation for IMUs supporting both FLIR and Eagle (warning – these .csv files each have several million lines and conventional spreadsheet programs may not accommodate them conveniently).

<i>Filename</i>	<i>description</i>
230105_232341_rt135_diff_250.kmz	KMZ nav metadata, FLIR, 230106 day
230105_232341_rt135_diff_250.csv	Full (250Hz) nav data, FLIR, 230106 day
230106_114131_rt135_diff_250.kmz	KMZ nav metadata, FLIR, 230106 night
230106_114131_rt135_diff_250.csv	Full (250Hz) nav data, FLIR, 230106 night

The navigation metadata kmz files described above include the flight tracks themselves, both in 3-D and as a vertically-projected ground track, as well as regular placemarks showing the altitude and the time (in UTC seconds-of-day). If viewed in Google Earth, only the ground track is visible by default on opening, but the other data can be selected on or off by unfolding the KMZ folder structure. The following table shows the approximate local time (Australian Central Daylight Time, ACDT) for the middle of each flight line, day and night, with reference to the flight line numbers shown above.

Flight line (ref illustration 2)	Midpoint time (ACDT)	
	Day	Night
1	1108	2317
2	1113	2324
3	1120	2336
4	1128	2345
5	1137	2354
6	1149	0005
7	1157	0014
8	1208	0025
9	1217	0034
10	1225	0045
11	1235	0057
12	1244	0108
13	1253	0116
14	1302	0127
15	1309	0135
16	1318	0143
17	1325	0150
18	1334	0159
19	1341	0205
20	1348	0212
21	1355	0218
22	1403	0224
23	1410	0229
24	1413	0233
25	1419	0238
26	1424	0243
27	1429	0248
28	1438	0253
29	1442	0257
30	1455	0300

7.Data validation and context

As described above, thermal imagery data was collected across four days with combined daytime/nighttime flights on the 18th, 19th, 26th of March and the 16th of April 2022.

7.1.Synoptic situation

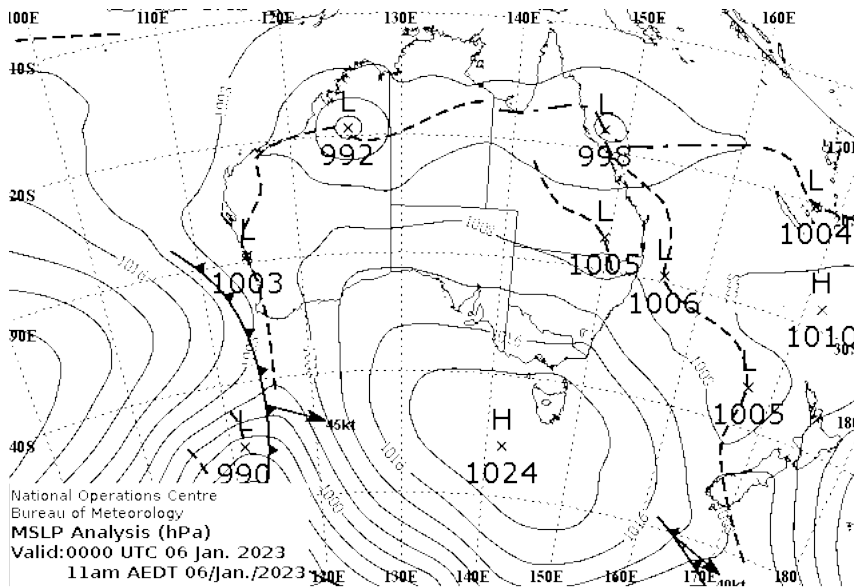


Illustration 3: Synoptic situation for the day of the flights (BOM).

Similar to the days of data capture in 2022, this displays a high pressure system to the south-east which results in weak northerlies to north-easterlies, ideal conditions for the development of an urban heat island.

7.2. Comparison data

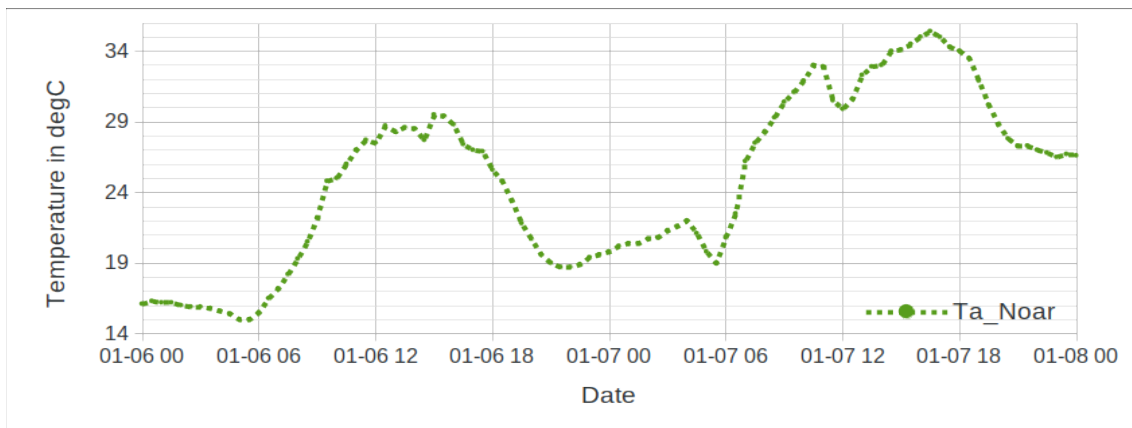
Several data sources were identified to compare and validate the surface temperature measurements from the airborne thermal imagery. This southern subregion includes a BoM automatic weather stations at Port Noarlunga, which provide time series of air temperature measurements as well as other meteorological parameters. This data is assimilated into the operational forecasting and analysis models to provide high resolution (12km) air temperature analyses

(<http://www.bom.gov.au/nwp/doc/access/NWPDData.shtml>). We note that air temperature is not expected to be a close match to the surface temperature although some degree of interrelation is anticipated.

7.3. Australian Bureau of Meteorology Automatic Weather Stations

Five of the BoM's automatic weather stations (AWS) fall inside the overall study area although only one lies in the southern subregion described in this Part B of the report. Its temperature measurements (in a Stevenson Screen, mounted 1.2m above ground) are shown below for the periods of all the flights covered by this report.

- 10: NOARLUNGA
 - latitude: -35.1586, longitude: 138.5057, height: 55.0 m



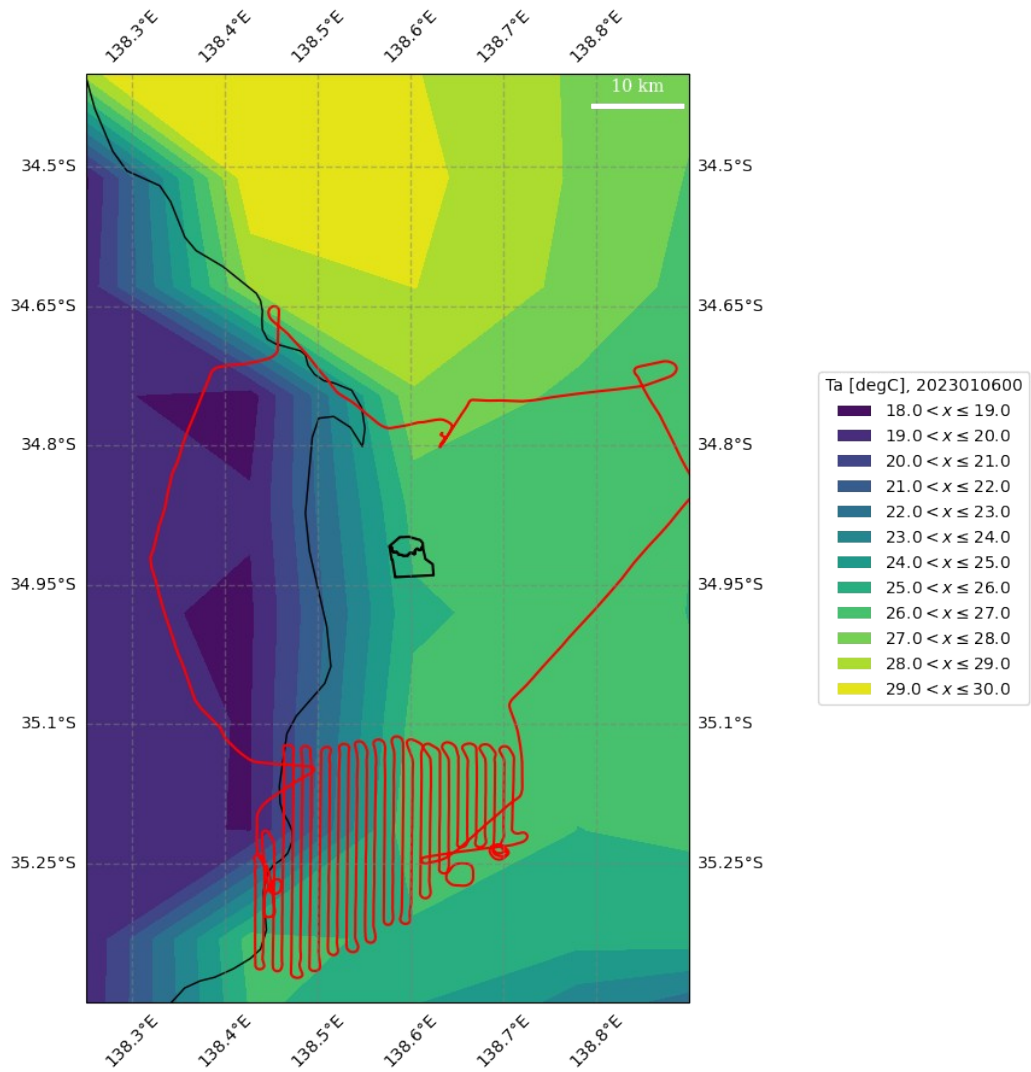
7.4. Australian Bureau of Meteorology ACCESS-G Model output

As noted previously, the BoM assimilates data from its entire AWS network and other sources into the operational forecasting and analysis model ACCESS-G to provide high resolution (12km) air temperature analyses valid across the whole country (<http://www.bom.gov.au/nwp/doc/access/NWPDData.shtml>). This provides air temperature data extending the area across which the AWS station measurements can be compared with other datasets.

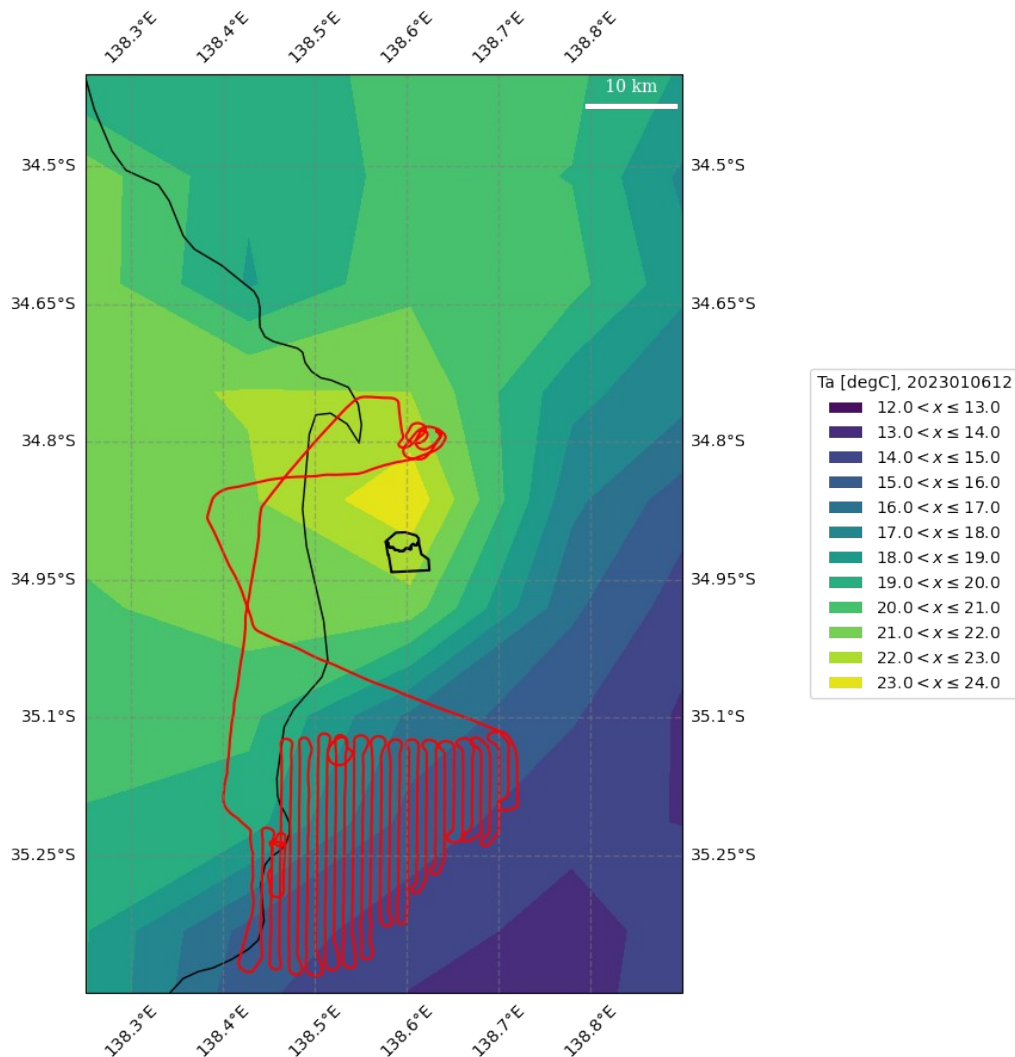
The following pages show this air temperature analysis data relevant to all of this

project's measurement flights, overlaid with the matching flight tracks.

6th January 2023: daytime flight, 0300 UTC (1330 ACDT)



6th January 2023: nighttime flight, 1500 UTC (0130 ACDT)



7.5. Assessment of Thermal accuracy

The comparisons described in both parts of this report between the radiometric brightness temperatures measured by ARA and independent sources of measured air temperatures and of satellite-based thermal imagery give a very large number of comparison points to assess the agreement of the datasets with agreed “standard” products.

The satellite-based data is particularly useful for assessing the accuracy of this project’s thermal data because it measures the same quantity (radiometric brightness temperature) and is widely used across the world with a high degree of ongoing intercomparison with other independent scientific datasets.

Although the restricted number of available suitable satellite overpasses meant that no exactly simultaneous measurements were made, there were quite close passes as discussed in the relevant sections of the first part of the report (“Radiometric comparison datasets”, pages 40 to 49). The lack of simultaneity adds the unknown change in physical temperature between the airborne observations and the reference satellite datasets, which is expected to be less than approximately two degrees based on the AWS-observed rates of change of temperature.

It is therefore gratifying to see residual differences between the absolute values of airborne observations and the reference satellite data of 0.8 K (50th percentile), with 95% of comparison points within 2.5 K. We would expect comparison with an actually simultaneous overpass to have even smaller residuals.

Local area consistency of airborne thermal imagery across small numbers of pixels supports local relative accuracies at the limits of the raw data resolution, i.e. better than 0.1 K.

We note that the manufacturer’s FLIR A615 thermal imager instrument specifications (Appendix 1 of the first part of the report) indicate an expected absolute accuracy of $\pm 2^{\circ}\text{C}$, which is consistent with our analysis.

Residuals (degrees C)	
Mean (before zeroed)	-0.386
Standard deviation	1.33
Minimum	-23.2
Maximum	15.2
50th percentile (absolute value)	0.799
75th percentile (absolute value)	1.38
95th percentile (absolute value)	2.51